CHAPTER 1

Introduction

The ultimate goal for oil and gas companies is to produce hydrocarbons in a sustainable and economically viable manner. Considering that many mature fields are now facing a decline in production and the exploration of new reserves is consistently more challenging, the industry demands optimization (Veeken, 2007). It finally became clear that, in order to understand the complexity of a reservoir and the petroleum system as a whole and thus produce solutions to overcome these new challenges, using all piece of information available was of paramount importance. In the last two decades, this has brought together professionals from many fields, such as Geology, Geophysics, Petrophysics and Engineering. After all, the different types of information addressed by each of these areas are complementary in nature, which highlights the importance of establishing links between different disciplines (Boyer and Mari, 1997).

Seismic data has been largely used in the oil and gas industry due its capacity of providing information regarding geometry and depth of reflectors below surface. However, with advances in technology – especially computer power – new methods have been developed for obtaining more information about the subsurface geology. As a seismic pulse propagates down through the stratigraphic layers, its amplitude is modified at each interface. This change in amplitude is controlled by the contrast in Acoustic Impedance (AI), which is the product of bulk density and velocity (Veeken, 2007). The seismic amplitudes can then be used to obtain relative acoustic impedance between the different layer boundaries through the process known as Seismic Inversion (Russel, 1991). These acoustic impedances when correlated with wellbore data allow the interpretation to be extended three-dimensionally throughout the seismic volume. Besides, while the seismic data covers a large volume but with limited vertical resolution (tens of meters), the well data – although limited to the wellbore surroundings – presents very high vertical resolution (tens of centimeters). Thus, insight into the reservoir properties is gained once the inversion results are correlated with rock physics and petrophysical models to infer lithology, porosity, presence of fluids as well as other geomechanical parameters (Simm and Bacon, 2014).

Inversion methods are classified into two main categories, deterministic methods and probabilistic/stochastic methods. Deterministic inversion algorithms try to minimize the difference between a modelled seismic trace and the actual seismic trace. It results in a smoother solution for the problem, which represents a best estimate given the limitation of the data’s frequency content (Oldenburg, 1983; Cookea and Cant, 2010). Due to the bandwidth limitation, there are several solutions that would satisfactorily match the seismic trace (non-uniqueness). Additionaly, the presence of thin beds, volume calculation and reservoir connectivity may be biased by the inherent smoothed solution produced by deterministic methods (Sancervero *et al.*, 2005). In practical terms it means that in geological layers of less than ¼ of the seismic wavelength, inversion results might be unreliable for quantitative interpretation. In order to address these problems, Simm and Bacon (2014) mention stochastic inversion as a proper way to deal with the non-uniqueness problem of the sub-tuning component in seismic data once it uses a smaller sampling increment as well as it attempts to describe the potential variability of inverse solution. Yet, because each realisation of the model matches the seismic trace, geostatistical variations between the wells are honoured and it ties the wells exactly (Veeken and da Silva, 2004). Hence after a certain number of realisations, the mean is close to the best-estimate inversion, but now the full range of uncertainty is approached.

Stochastic inversion differs from all other methods in one aspect. It does not use an objective function and hence a simplicity term to stabilize the solution is not needed. Instead, property solutions like impedance and porosity, for instance, are drawn from a probability density function (pdf) of possible outcomes, i.e. these outcomes are constrained by acceptable values (Russell and Hampson, 2006). Since the simulations can be done at arbitrary sample intervals, close to the wells high resolution can be reasonably inferred and away from the wells the absence of a simplicity term along with the statistical conditioning still makes it possible to achieve resolution beyond traditional inversion methods (Bosch *et al.*, 2010). A *priori* information for the inversion process is provided by the well-log, which it is assumed to be the correct solution. The probabilistic inversion algorithm simply accepts or discards simulations at individual grid points depending upon whether they imply synthetics which agree with the input seismic (Simm and Bacon, 2014). Whether a given simulation is accepted or rejected can be alternatively controlled by incorporating a simulated annealing strategy (Cookea and Cant, 2010). This inversion option results in a tighter set of simulations where the full distribution can then be used to estimate risk or make probability maps.

1.1. Study Area

The Maari Field sits 80 km off the South Taranaki coast, in the southern portion of Taranaki Basin, New Zealand (Figure 1.1). Discovered by the Moki-1 exploration well in 1983, Maari covers an area of approximately 80 km^2 and is currently the New Zealand's largest oilfield (OMV, 2017). Recoverable reserves in the Maari-3D area were first estimated to be 50 mmbbl of oil but additional discoveries in the Manaia prospect have recently doubled the field reserves (NZPM, 2014). The field produces mainly from the Moki Formation (Miocene age, ~17-13 Ma), a submarine fan deposit (coarse-grained sands) presenting thicknesses of 250 to 350m, porosities of 15 to 26% and permeabilities up to 98 mD. Additional accumulations do occur in younger M2A and older Eocene (~56-34 Ma) Kapuni Group sands. The hydrocarbons are trapped in N-S trending closures formed by Neogene (~24-05 Ma) shortening (King and Thrasher, 1996).

Despite the discovery still in the early 80's, it took over twenty years to make the final development decision. Due to moderate reservoir quality in the field, artificial lift and water injection for pressure support are required (NZPM, 2014). Finally, the well Maari-1A proved that successful production could be achieved from horizontally-drilled wells. Drilled to test the Moki Formation sands, the horizontal-sidetrack well produced 4,370 bopd on test. Of the 664 m drilled along the Moki Formation, 563 m were oil-bearing, with an average porosity of 24% and oil saturation of 75% (Halliburton/Shell, 1999). Production started in 2009 and since then, more than 30 million barrels of oil have been produced from the field. A total of ten production and injection wells are currently hosted by a wellhead platform, the WHP Tiro Tiro Moana (OMV, 2017). The

Maari offshore production site also contains an FPSO vessel (Raroa II), anchored 1.5 km from the platform and with a storage capacity of 590,000 bbl, production capacity of 40,000 bopd and water injection capacity of 40,000 bwpd (NZPM, 2014).

1.1.1. Geological Setting and Tectonic History

The Taranaki Basin is a mostly offshore sedimentary basin located along the west coast of the North Island, New Zealand (Figure 1.2). The basin likely had its origin during the late Cretaceous Taranaki Rift (~85-80 Ma), after the breakup of the Gondwana supercontinent. Later, during the Cenozoic, it experienced several other geological processes: subsidence, compression, additional rifting as well as strike-slip faulting, all commonly associated with previous rift-controlling faults being reactivated (Thrasher, 1992). In fact, the basin's tectonic evolution can be divided into four different phases: Rifting, Drift, Foreland Basin Development and Intra-Arc Basin Development (Baur *et al.*, 2014).

First, syn-rift deposition occurred within grabens across the basin; a regional unconformity separates these sediments from the basement. Higgs *et al.* (2012) point out that during the Drift phase, Paleocene-Eocene Sandstones (~65-35 Ma) – which today configure the main reservoirs found within the basin – were being deposited while the basin went through a marine transgression event. In the Oligocene (~34-23 Ma), a change from a passive margin to a foreland basin was caused by subduction of the Pacific Plate under the Australian plate. Stresses were then reoriented and there was reactivation along normal faults resulting in strike-slip faulting (Palmer and Geoff, 1988). Finally, during the mid to late Miocene (~15-05 Ma), multiple-strike-slip and reverse faults are generated as the subduction (involving Pacific and Australian plate) continued along with the movement of the plate boundary, which ended up reallocating stresses in the basin (Kroeger *et al.*, 2013).

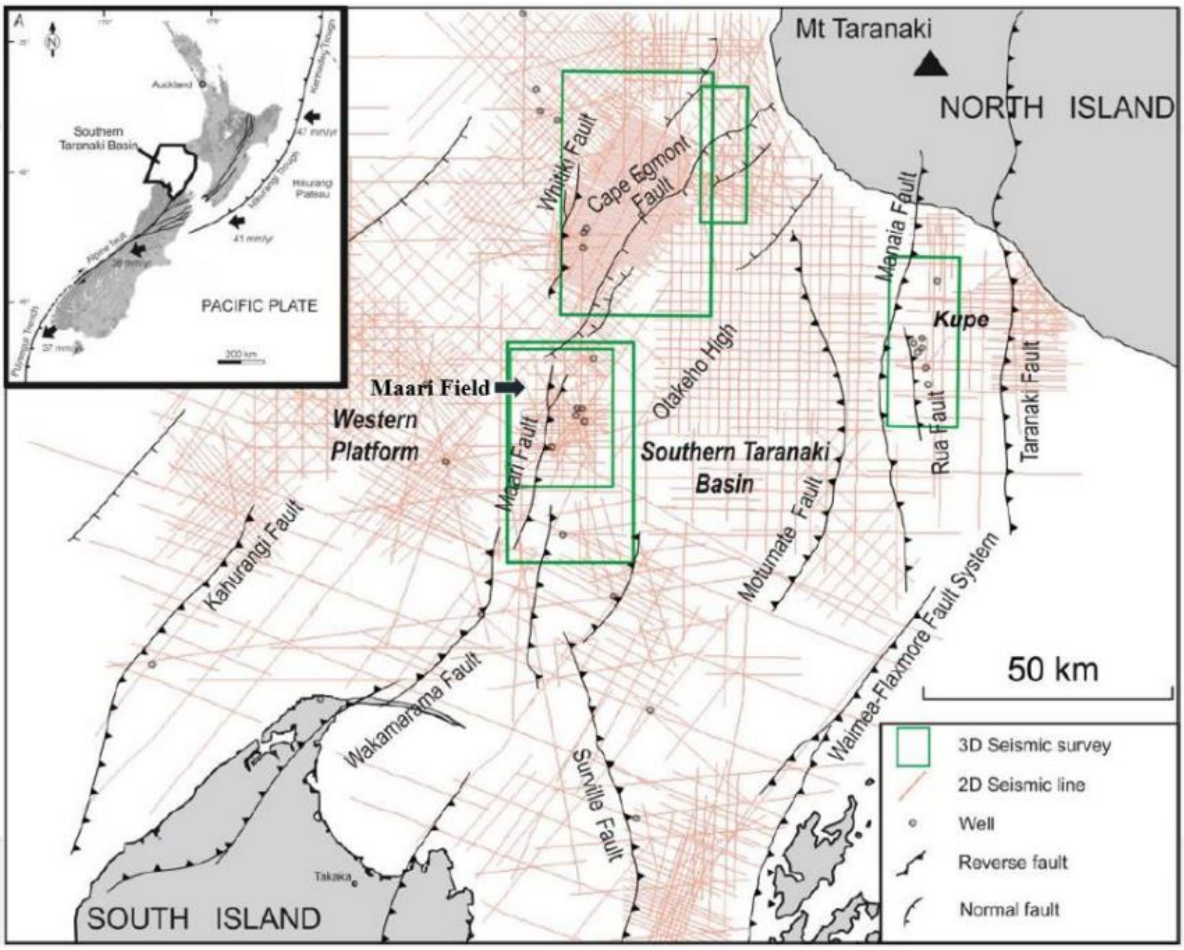

Figure 1.1: Location of Maari Field in the Taranaki Basin, New Zealand (Reilly *et al.*, 2014)

Due to New Zealand's recent tectonic setting (Oligocene/Miocene to date) along an active plate margin – where the Pacific plate subducts beneath the Australian Plate – Taranaki's structure has been strongly affected by major changes in direction and amplitude of stresses (Pilaar and Wakefield, 1978). Changes in this plate boundary, according to King (2000), affected not just the geometry, but also basin's subsequent infill and therefore the petroleum systems present today at Taranaki. The basin can be divided into three structurally distinct units with base on their prevailing deformation style. Knox (1982) asserts that these units are an expression of regional, yet time-distinct, tectonic events that are currently distinguished in the west, north and southern parts of the basin (Figure 1.3). The Western Unit (or Western Platform), which is more than 200 km wide in some places, has remained stable since Late Eocene time (~38-34

Ma) and therefore presents relatively simple structures with up to 5 km of sedimentary layer thickness (Palmer, 1985). The Northern and Southern Units, on the other hand, have been largely affected by Late Miocene-Recent tectonic events. While the Southern Unit is characterized by reverse faulting and inversion, the Northern Unit has undergone normal faulting and extension with continuous subsidence (Knox, 1982).

Among all New Zealand's known hydrocarbon reserves, Taranaki Basin holds the most prolific oil and gas fields (Thrasher, 1992). Historically, exploration in Taranaki has targeted mainly four-way dip closures, rotated fault blocks, foreland folds and detached thrust sheets along the eastern part of the basin (NZPM, 2014). Over 400 exploration and production wells have been drilled to date and the basin currently produces from about 20 fields. In this context the southern unit (Figure 1.2) – where the Maari, Maui and Tui fields are located – stands out being responsible for almost 70 percent of the New Zealand's oil production or almost 180 million Barrels of Oil Equivalent (BOE) annually (Palmer and Geoff, 1988). Despite all that has been previously mentioned here, the Taranaki Basin is still considered under-explored compared to similar basins of its size. With no exploration records beyond the shelf thus far, there remains a considerable potential for further commercial hydrocarbon discoveries (NZPM, 2014).

1.1.2. Taranaki Basin Stratigraphy

King and Thrasher (1996) proposed the following subdivision to the Taranaki Basin stratigraphy (Figure 1.4):

I. Late Cretaceous syn-rift sequence (Pakawau Group);

II. Paleocene-Eocene late-rift and post-rift transgressive sequence (Kapuni and Moa Groups);

III. Oligocene-Miocene fore-deep and distal sediment starved shelf and slope sequence (Ngatoro Group) and Miocene regressive sequence (Wai-ti Group);

IV. Plio-Pleistocene regressive Sequence (Rotokare Group).

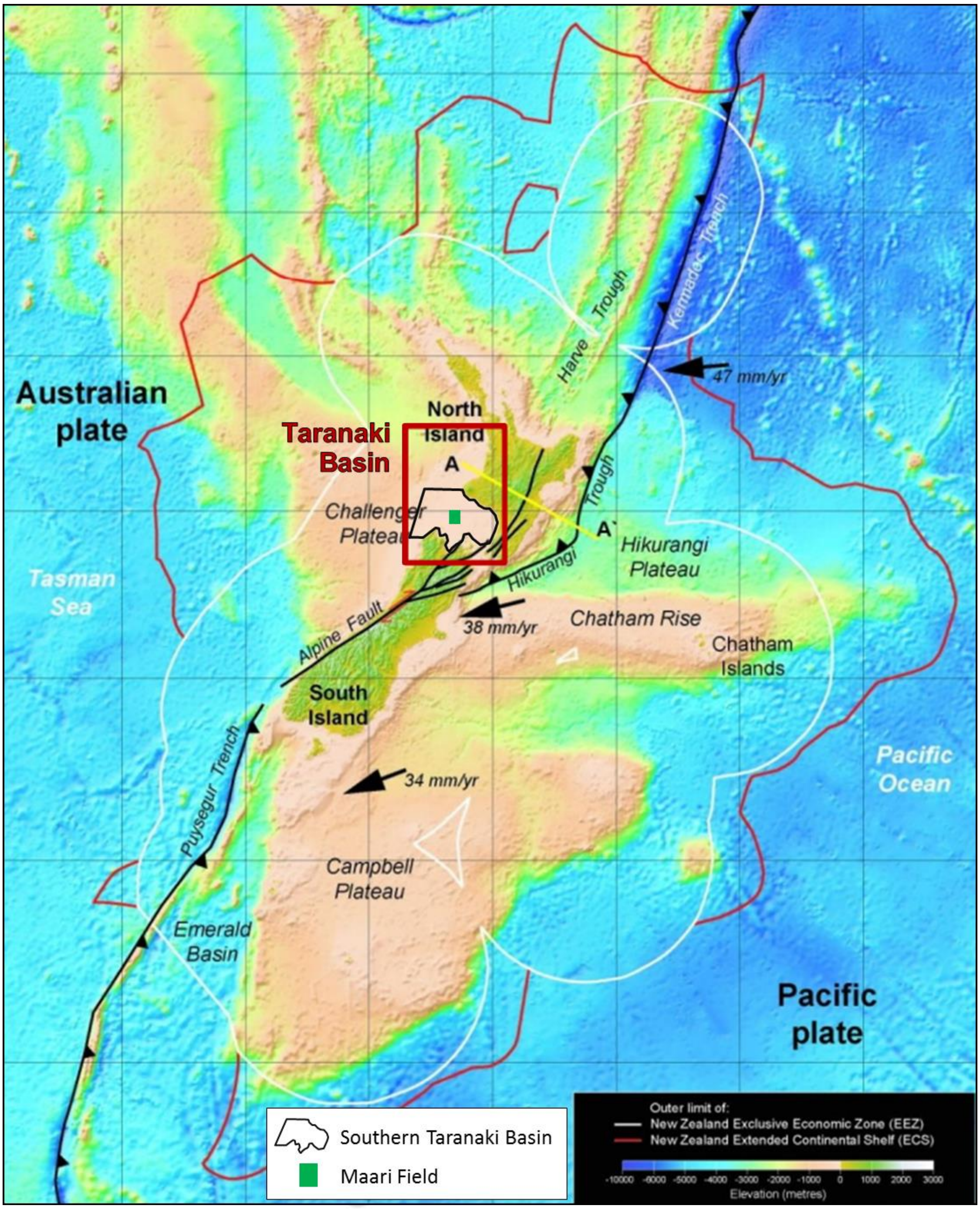

Figure 1.2: New Zealand's regional setting. The Taranaki Basin currently sits above an active plate margin, where the Pacific Plate is subducting beneath the Australian Plate (modified from Strogen *et al.*, 2012)

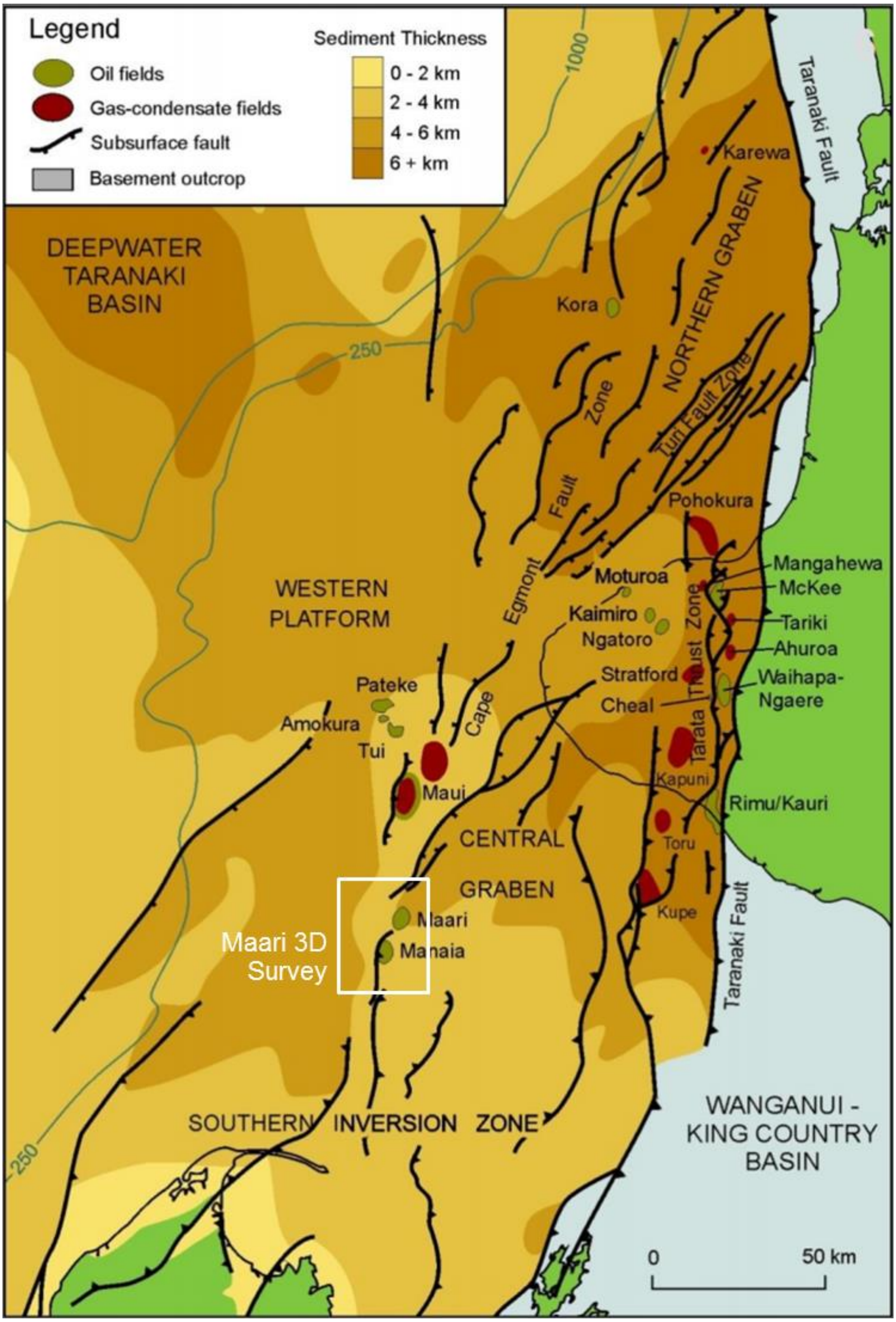

Figure 1.3: Structural Units and producing oil and gas fields present in the Taranaki Basin. Note how the Maari oil field is located in the Southern Inversion Zone (modified from NZPM, 2014)

At an early stage – late Cretaceous (~85-80 Ma), syn-rift deposits associated to the break-up of the supercontinent Gondwana occurred along the entire basin. During that stage, thick deposits of up to 6 kilometers were deposited in the Southern Taranaki (King and Thrasher, 1996). The period is characterized by terrestrial sediments – interbedded coals and sandstone sequence – deposited in the Pakawau Group. From that period on, sedimentation at the Taranki Basin was mainly controlled by sea level fluctuations, i.e. trangressive-regressive sequences (Nodder, 1993).

Paleocene and Eocene (~65-35 Ma) sediments configure a terrestrial to marginal marine sequences (Kapuni Group) as the sea transgressed over the entire region. Some of the most important reservoirs of the basin were deposit at this time. During the Oligocene (~34-23 Ma), a decrease in clastic deposition resulted in limestones and calcareous mudstones comprising the Otaraoa, Tikorangi and Taimana formations throughout the basin. At the time, clastic sediments were limited to deposits that today configure the Ngatoro Group (Palmer, 1985). The period is followed by a major change in the basin tectonic regime. Stresses are reallocated at the early Miocene (~23-15 Ma) as the proximity between the basin and the active subduction zone between Australian and Pacific plate increases (Kroeger *et al.*, 2013). This results in a massive supply of clastic material which end up being deposited to the west of the Taranaki Fault (see Figure 1.3 for location). These deposits are predominantly bathyal mudstones, with thickness surpassing 1 kilometer at some locations, known today as the Manganui Formation (Pilaar and Wakefield, 1978). The bathyal mudstone is just partially interrupted by layers of interbedded sandstones and siltstones that mark the turbitide reservoir of the Moki, Mount Messenger and the M2A formations of the Wai-iti Group (Grain, 2008). From the mid Miocene to Pliocene (~15-05 Ma), the basin experienced a further extension (Knox, 1982). The extensional regime now co-occur with volcanic activities; it is predominant at the Northern and Central Graben, resulting in the Mohakatino Volcanics: a chain of submarine andesite stratovolcanoes and associated intrusive complexes (King and Thrasher, 1996). In the same period, the Rotokare Group – large clinoforms known as the Giant Foresets Fm. – was being deposited, configuring a sediment wedge prograding towards northwest (Thrasher, 1992).

The stratigraphy at the Maari area can be summarized looking at the well Maui-4, the only well at the area which penetrated the entire column of sediments reaching the basement at a measured depth of ~3840 m below Kelly Bushing. A brief description of the stratigraphy at this well will be presented below, from older to younger units, with emphasis at the main reservoir in the Maari area – the Moki Fm.

1.1.2.1. Pakawau Group (Late Cretaceous)

At an early stage, the extensional setting modeled the basin with a typical rifting topography consisting of downfaulted grabens with intervening basement horsts (Knox, 1982). These grabens started to be filled at the middle-late Cretaceous (~80-66 Ma) predominantly by coarse facies, including non-marine conglomerates and coarse sandstones along with mudstones and coals that constitute the Pakawau Group (Pilaar and Wakefield, 1978). All these sediments had provenance from nearby basement lithologies and were deposited in packages up to 4000m thick (King and Thrasher, 1996).

Evidences from wells drilled at the northern part of the basin show that the marine influence gradually increases northwards (de Bock *et al.*, 1991). The Group was then divided into the Rakopi Fm., dominated by coal measures, and the North Cape Fm., which is dominated by shallow marine lithofacies. This subdivision is supported by different sources of data, such as seismic reflection mapping, lithofacies character from wells and geochemical data (Palmer *et al.*, 1988). Lithofacies in the Rakopi Fm. are indicative of swamp and fluvial food plain environments, whilst the North Cape Fm. was deposited in shallow marine, paralic and terrestrial settings (King and Thrasher, 1996). The contact between Rakopi and overlying North Cape Fm. is marked by a transgression, which sometimes can be seen on seismic as a mild unconformity (Thrasher, 1992).

1.1.2.2. Kapuni Group and Moa Group (Paleocene-Eocene)

Following a marine transgression that marked the late Cretaceous, the Pakawau Group is overlain by two groups: the Kapuni Group, containing terrestrial to marginal marine sediments, and the Moa Group, entirely marine. In fault-bounded depocentres, these two groups configure a sequence that can sometimes be as thick as 2000m (King and Thrasher, 1996). Unlike the Pakawau though, Kapuni Group sedimentation was not restricted to grabens depocentres and consequently it is widely spread at Taranaki. In fact, they configure a stratigraphic interval between top Cretaceous (~66 Ma) and top Eocene (~34 Ma) horizons which are mappable throughout the basin (Thrasher, 1992).

The Kapuni Group comprises the formations Farewell, Kaimiro, Mangahewa and Mckee. They are mainly constituted by sandstones, mudstones and coals. It is the producing unit for many fields in the Taranaki Basin, both onshore and offshore (Palmer *et al.*, 1988). Paleogeographic studies support the idea of a southeastwards transgression from the late Cretaceous to early Miocene (~66-34 Ma), which occurred intercalating high fluctuations of the sea level with nearly constant periods (de Bock *et al.*, 1991). During the quiet episodes, quite thick sandstone deposits occurred along the coastal zone (King and Thrasher, 1996). Still, as reservoirs, the sandstones within the Kapuni Group present grand variation in reservoir quality (Palmer *et al.*, 1988). Normally it depends greatly on the depositional environment and depth of burial. At the well Maui-4, for example, a petrophysical evaluation of the interval associated to the Mangahewa formation (Kapuni Group) indicates an average porosity of 14% and permeability (k) of 5.5 mD with water saturation of 38%. On test, the formation flowed 575 bopd (de Bock *et al.*, 1991).

The Moa Group refers to marine correlatives of the Kapuni Group, which include a series of fine-grained, calcareous siltstones and sandstones (Palmer, 1985). It includes two different formations, referred to as Turi and Tangaroa Fm. The Turi Formation is predominantly a non-calcareous, dark colored, carbonaceous, marine mudstone deposited in shelf and bathyal regions. The Tangaroa Formation consists of a sequence of deep marine sandstones (fine-to-coarse grained) separated by a thin limestone (King and Thrasher, 1996). These sediments were very likely deposited by debris flows and turbidity currents as seismic reflection mapping reveal a fan lobe geometry with an interval morphology marked by progradational wedges (Gresko *et al.*, 1992).

1.1.2.3. Ngatoro Group (Oligocene-Early Miocene)

The group is divided into three different formations: Otaraoa, Tikorangi and Taimana. Rocks from the period that goes from Oligocene to early Miocene (~34-23 Ma) normally have a high calcium carbonate content. Despite the fact that carbonate sedimentation is generally associated with tectonic stability and low rates of terrigenous input, deposition of the Ngatoro Group coincided with a major change in Taranaki's tectonic regime (King and Thrasher, 1996). The period marks an accelerated marine inundation associated with renewed subsidence.

The Otaroa Formation is defined as a sequence of calcareous siltstones and sandstones deposited in outer shelf to bathyal water depths and that is well developed onshore (thickness up to 1200 m), but that offshore is less than 100 meters thick (Palmer. 1985). The Tikorangi Fm. is a bioclastic limestone sequence that is widespread in Taranaki Basin and configures a regional seismic marker (de Bock *et al.*, 1991). In the southern part of the basin, well developed chalk and marl within the Tikorangi limestone indicates deposit in a transition zone between the platform and basinal carbonate facies (King and Thrasher, 1996). The Taimana Fm. is characterized by a highly calcareous interval (mainly argillaceous limestones and marls), generally less than 250m thick, deposited near the maximum extent of a regional transgression. It overlies the Tikorangi Formation and the contact between these two formations is disconformable in several places (Palmer, 1985).

1.1.2.4. Wai-ti Group (Miocene)

The Wai-ti Group is an entirely marine, regressive, clastic dominated succession that is divided into six formations: Manganui, Moki, Mohakatino, Mount Messenger, Urenui and Ariki. In the southern part of the basin, Miocene (~23-05 Ma) sediments are preserved in the downthrown side of inverted anticlines, where they may be as thick as 2000 m (King and Thrasher, 1996). The sequence includes (1) mudstones and siltstones of the Manganui Formation, (2) sandstone-dominated turbidite sequences of the Moki and Mount Messenger formations, (3) slope siltstones of the Urenui Fm., (4) deepwater volcanoclastics of the Mohakatino Fm. and (5) basin floor marls of the Ariki Formation (de Bock *et al.*, 1991). Tectonically, the period is associated to widespread reverse faulting due to compressional regime commenced in the South Taranaki Graben.

The Manganui Fm. is distributed basin wide and dominates the Miocene succession along the basin. The formation can be up to 1700m thick in some particular areas of the basin, which makes it convenient to subdivide the formation into 'upper' and 'lower' Manganui. The term Lower Manganui is used to distinguish the interval between the Taimana and Moki Formations from the 'upper' Manganui overlying the Moki formation. The deposition occurred at bathyal depths across most of the Taranaki Basin during the Early Miocene (~23-16 Ma). Southernmost parts of the basin were at shallower depths throughout the period and normally present coarser grains than elsewhere (King and Thrasher, 1996).

1.1.2.4.1. Moki Formation

The Moki Fm. consists of sandstone interbedded with mudstone, siltstone and minor limestone. The formation is part of a submarine fan deposit presenting thicknesses of 250 to 350 meters. It represents the first main influx of clastic sediments deposited on the deep basin floor during the lower middle Miocene (~15 Ma). The sequence was built up by turbidite deposits and was widely deposited across the Taranaki Basin (Thrasher, 1992). The sands were mainly derived from the south and south-east, a conclusion based on regional paleogeography reconstruction and patterns of sandstones distribution in wells (King and Thrasher, 1996). An attractive feature of the Moki Fm. sands is that, generally, it is buried to less than 3000 m, which significantly improves the likelihood of preservation of primary porosity and permeability (Palmer *et al.*, 1988).

The thin to thickly bedded sandstones are typically very fine to fine-grained, and are commonly argillaceous Thick, fine to coarse-grained, upward coarsening sandstones sequences, channel sandstones and pebbles bands occur locally (de Bock *et al.*, 1991). Sandstone quality and thickness within the Moki is widely variable and generally unpredictable. The relative position of the wells on the paleo-fan system can be important for predicting reservoir geometry and continuity (Palmer *et al.*, 1988). For example, fans are thicker at the apex and thinner at the outer margin. Also, the inner fan can build up levees that are tens of meters above the fan surface (Walker, 1978). According to the well completion reports, in Maui-4, Moki Fm. sandstone is described as very fine to fine-grained; Moki-1 well shows very fine, occasionally medium-grained, usually argillaceous sands; and in Moki-2A, it is described as fine to coarse, friable to loose with generally good visible porosity. Most of the wells drilled to date are considered to be in a mid-fan (supra fan) position (de Bock *et al.*, 1991).

1.1.2.5. Rotokare Group (Pliocene-Pleistocene)

The Rotokare Group is composed by the Matemateaonga, Tangahoe, Mangaa and Giant Foresets formations. It overlies the Wai-ti Group and the contact, particularly in the southern part of the basin, is pronounced as a visible angular unconformity on seismic reflection profiles (King and Thrasher, 1996). This unconformity was initially centred on individual inversion structures, but subsequently regional uplift also occurred, with greatest uplift towards the south, which caused differential erosion of older strata. Plio-Pleistocenes successions, consequently, are thick across the basin – except in the southern Taranaki.

The period is marked by a sequence of prograding strata as marine deposition continued through the Pliocene to the present as the continental shelf built out to the northwest. Deposition is associated to normal faulting during this time, with thick sediments deposited on the downthrown sides (de Bock *et al.*, 1991).

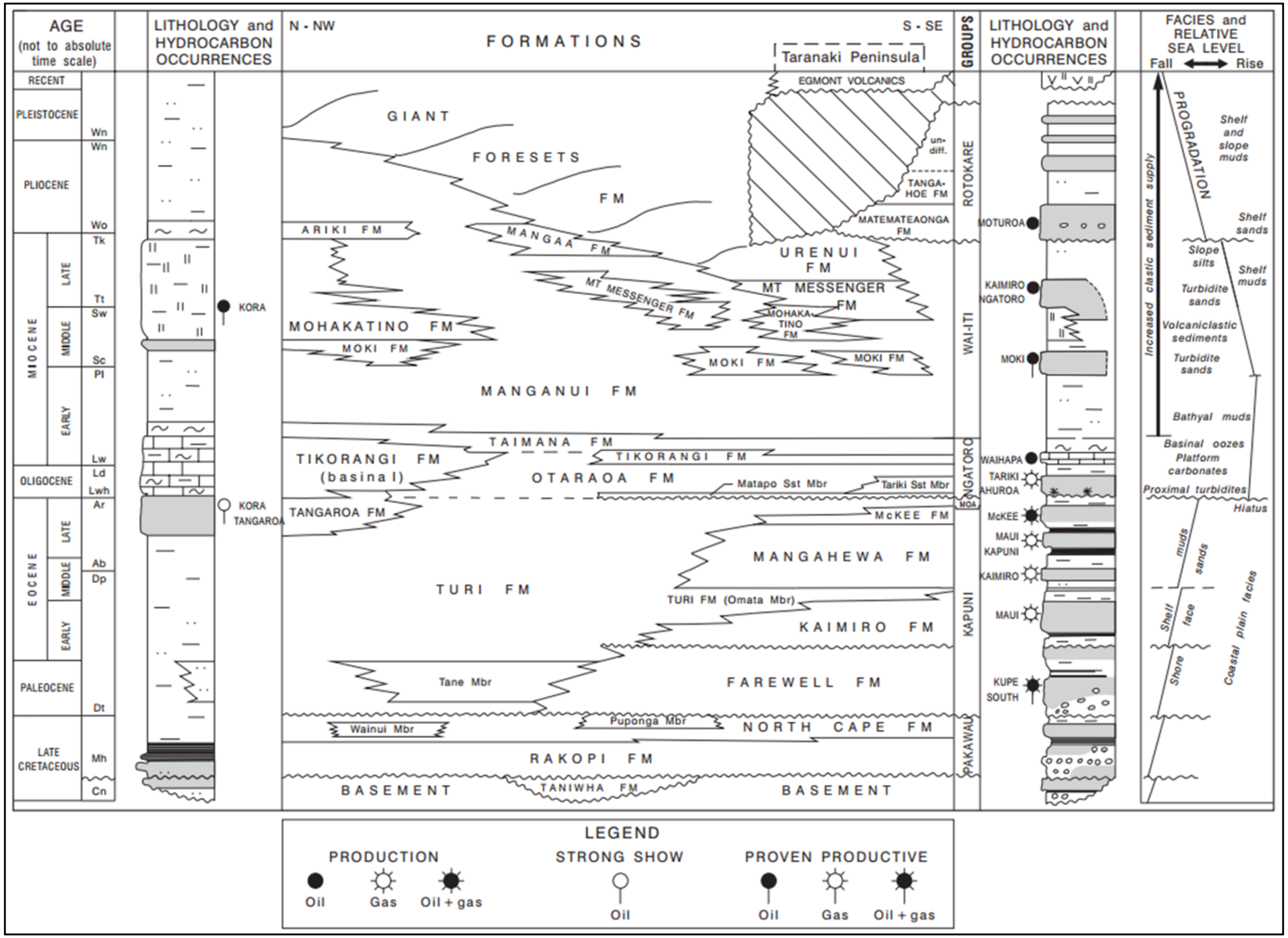

Figure 1.4: Generalized Stratigraphy of the Taranaki Basin (King and Thrasher, 1996)

1.2. 3D Maari Seismic Data

The 3D Maari Seismic Survey covers approximately 514 km^2 (27 km long, inline direction, by 19 km wide, crossline direction) of the Southern unit, offshore Taranaki Basin. The data was acquired by the Schlumberger Geco-Prakla Company using the vessel *M/V Geco Resolution* between 12 March and 14 April 1999. A sampling interval of 2 ms and a bin size of 25 m (inline) and 12.5 m (cross-line) were used to acquire the seismic data. After processing, the Maari 3D Seismic is available now as a full-stack seismic cube in SEG-Y format containing 1677 inlines (170-1846, step 2) and 2253 crosslines (379-2631, step 1) as can be seen in Figure 1.5. Polarity of the Maari 3D data is such that an increase in acoustic impedance (compression) is a trough (negative number). A summary of the seismic acquisition parameters used in the campaign can be found in Table 1.1. No obstructions or installations were located within the Maari 3D survey area.

According to the original report, the processing of the 3D Maari data had as objectives:

- Optimise resolution, signal-to-noise ratio, amplitude preservation, fault definition, continuity and structural imaging throughout the section;
- Retain relative amplitude information for AVO analysis and interpretation;
- Velocity analyses picked on a 500 x 500 meter grid.

Concerned about finding an optimal processing sequence for imaging the Maari's subsurface, the Maari participants OMV New Zealand Ltd (Operator, 69%) and Shell Todd Oil Services (STOS) (16%) actively participated in processing parameter decisions, reviewing tests and QC'ing every stage of the process. In the original report (Schlumberger/Shell, 1999 – p.31), Chapter 5.0 is entitled "Testing, Production and QC" and describes in detail, including examples of gathers/sections prior and post a determined process is applied, decision making and necessary explanations. For instance, it was decided that the 3D Maari data should be processed from start to end at the recorded sample rate of 2 ms, as it would bring improvements on high frequency amplitudes preservation. It also indicates the reason TAU-P Deconvolution was chosen over Wave Equation Demultiple (WED) to attenuate the multiple reflection generated by the sea floor; why trace interpolation in the CMP domain has been used before applying Parabolic Radon Demultiple; and explains the use of a new trace interpolation to bring post-stack row bin dimensions to 12.5 meters again in order to prevent steep structural dips from spatial aliasing before post-stack migration.

Table 1.1 – Acquisition Parameters from 3D Maari Seismic Data

Source Array Type	**Bolt Air Gun Array (5th Generation)**
Air Pressure	2000 Psi
Shooting Mode	Flip-Flop
Number of Guns per Array	8
Gun Depth	6 meters
Shot Point Interval	18.75 meters
Center Source Separation	50 meters
Number of Sources	2
Number of Streamers	6
Line Length (Full Fold)	25.10625 km
Total no. channels	1440 (6x240)
Number of Hydrophones per Group	12
Streamer Group Length	14.86 meters
Streamer Group Interval	12.5 meters
Streamer Separation	100 meters
Streamer Depth	7 meters
Active Streamer Length	6x3000 meters
Recording Length	6000 ms
Sample Rate	2 ms
Filter Setting	High Cut 200 Hz - 406 (dB/oct) Low Cut 3 Hz - 18 (dB/oct)

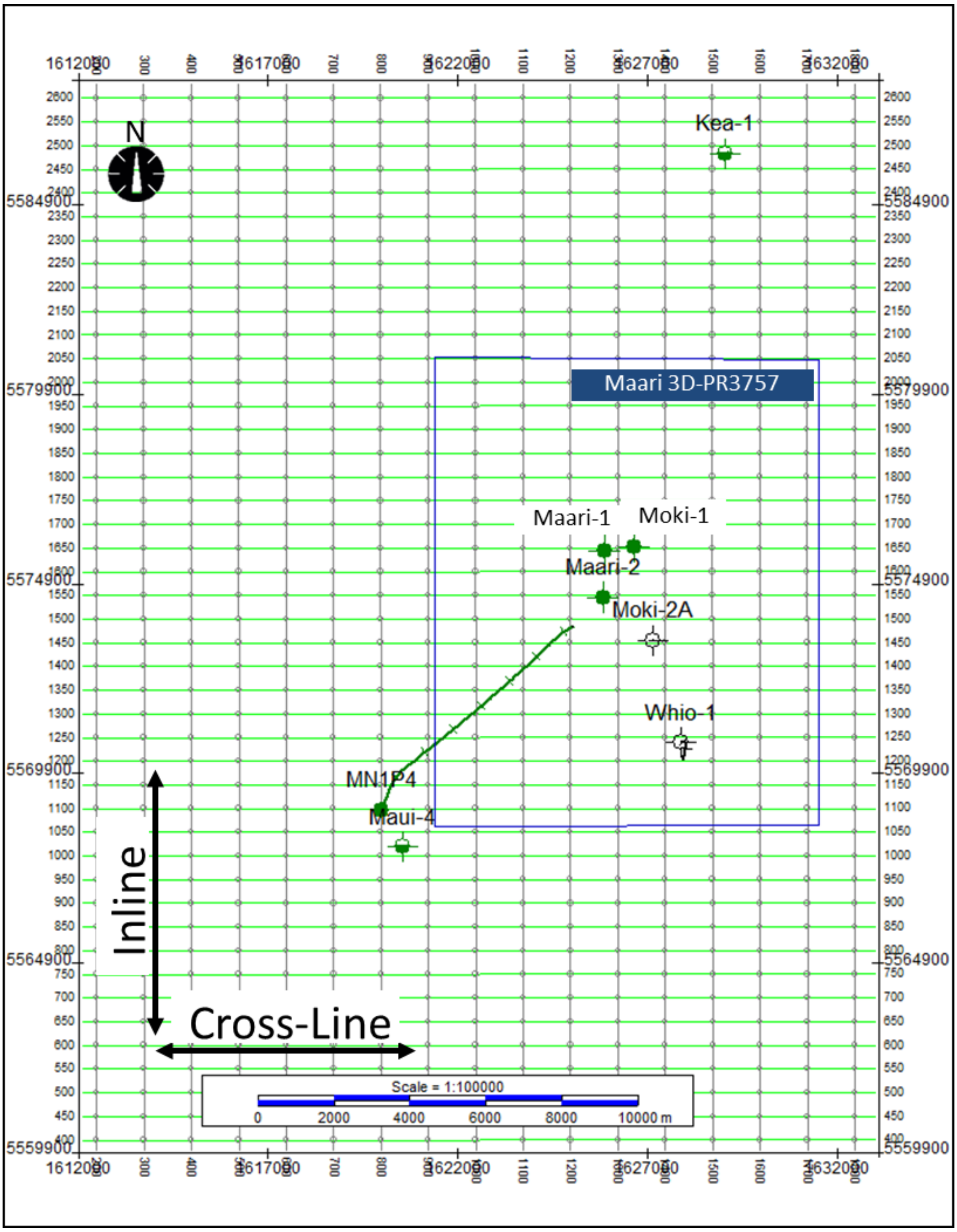

Figure 1.5: Base map of 3D Maari Seismic Data

Also, located in the Southern Inversion Zone (Figure 1.3), the Maari field is structurally complex. It presents high-angle faults and steeply dipping and folded structures, which are likely to be the cause of significant lateral velocity variations throughout the Maari area. A fine sampling at the velocity analysis procedure would be necessary in order to build a proper velocity field for applying radon demultiple and migration, for instance. Such abrupt lateral velocity changes may cause complications on relocating events at their true subsurface positions especially because, despite the structural complications, processing did not include pre-stack migration. Pre-stack migration is a relatively new method that may not had been available at the time due to lack of computer power required to run it in a 3D dataset. It is known that the use of a pre-stack migration algorithm could better focus energy at the right position for dipping events and non-zero offset traces as well as having higher signal/noise ratio compared to post-stack migration (Wu, 2001).

The data was then later reprocessed by CGG in 2001 (now including pre-stack migration) and the final reprocessing report was attached to the original report. This time, the report is quite specific when enumerating the problems standing on the way to the main objectives of (re)processing. The objectives are based on the previous experience gained when processing the 3D Maari data and are mentioned as follow:

- Improve the imaging in the problem areas. The problem areas are:
    - *Highly reflective overburden;*
    - *Areas with high structural dip;*
    - *Dense complex faulting;*
    - *Low velocity shallow gas anomalies;*
- Apply utmost attention to the field and prospect areas;
- Improve event continuity and time imaging;
- Ensure sharp fault imaging;
- Deliver dense and accurate seismic velocities for later depth conversion work;
- Process in true amplitude.

The pre-processing sequence (Schlumberger/Shell, 1999 – p. 110) included twenty-four steps, such as static shift, 3D geometry set, spherical divergence correction, swell noise attenuation, NMO removal, phase-only inverse Q filtering (Q150), Tau-P predictive deconvolution, Radon demultiple, etc. The final processing sequence was carried out through seven different Production and QC Phases, which involved many processing techniques being applied to the data. Exponential gain correction (8dB at 1000 ms – 16dB from 2000-6000 ms), zero-phasing filter application, Full Kirchhoff Pre-Stack Time Migration (PSTM), dense velocity field generation, final pre-stack NMO correction, 3D stack, random noise attenuation using FX projection filtering technique, inverse Q filter for amplitude deabsorption (Q540) and time variant filtering were just some of these procedures. Some of these steps with further description of the decision making process are highlighted at the end of the (re)processing report and a summary of these steps can be found below.

It was observed that regularisation of fold number by interpolation prior to PSTM resulted in better amplitude preservation through the migration process. In order to do that, a missing trace restoration was approached with an FX-Y interpolation. Also, during test parameters for the PSTM processing, a significant amount of noise in the data was considered responsible for a poor migration product. In order to improve the signal to noise ratio, CGG applied an FK anti-alias rejection filter with an optimum result obtained by rejecting outside K-Nyquist/2. Random noise from common offset planes was removed by using a FX projection filter technique that separates the signal assumed to be predictable in X from non-predictable noise for all the signal’s component frequencies. After that, tests were undertaken to decide the PSTM algorithm dip limitation and aperture size. The dip limitation value sets the maximum dip to be preserved after migration. Tests demonstrated that a dip of 40° imaged the steeply dipping faults without introducing any migration artefacts. The aperture size limits the spatial extension on either side of the migration trace of the migration operator. If limited too much, it leads to smearing. If too big, it requires extra computer power, which may compromise project’s time-frame. A 4000-meter aperture was used for the Maari migration. The improvement in signal-to-noise ratio prior to PSTM had as a consequence better migration results. Furthermore, it improved the dense velocity analysis which was later used to depth convert the data, producing the – also available – seismic volume Maari 3D-PR3757 (Figure 1.5). The velocity function picked at every bin location was smoothed and edited before it was included in the stacking-velocity field. A regression was applied in order to create a smooth function from the data by fitting a quadratic polynomial with weighted least squares.

A final stacked section of Maari 3D seismic data on cross-line 1650 is presented in Figure 1.6. The section crosses the wells Maari-1 and Moki-1, drilled on the crest of an anticline. From top to bottom, four horizons are shown: Pliocene unconformity, Moki Fm, Lower Manganui and Mangahewa. Note how some of the problems previously outlined, such as the presence of a highly reflective overburden and absence of amplitudes below possible shallow gas anomalies (eastern sector), can be observed. Also, the abrupt change in amplitudes (red arrow, western side of the anticline) is caused by the presence of a major positive inverted fault. This fault is poorly imaged (see Section 1.2) because its strike direction (SSW-NNE) nearly coincides with the direction that the seismic survey was shot (N-S, Inline). Figure 1.7 shows a time-slice at 850 ms TWTT, just below the Unconformity (yellow horizon, Figure 1.6), which illustrates the large area with a lack of amplitudes due to a poor imaging of the fault.

The presence of shallow gas anomalies over the Maari 3D area has recently been discussed in the literature. These gas clouds are known to be the cause of many dim amplitude areas around the field. Singh *et al.* (2016) used an artificial neural network to map gas migration pathways from the source rock to the shallow section. They, thereby, contributed to the understanding of the petroleum system, while attempting to prevent shallow hazards in future drilling campaigns. Figure 1.8 shows a dip-steered median filter (DSMF) section on inline 793 with low amplitudes associated to gas chimneys interpreted by Singh *et al.* (2016). Note how they look similar to the red dashed ellipse in the eastern part of Figure 1.6.

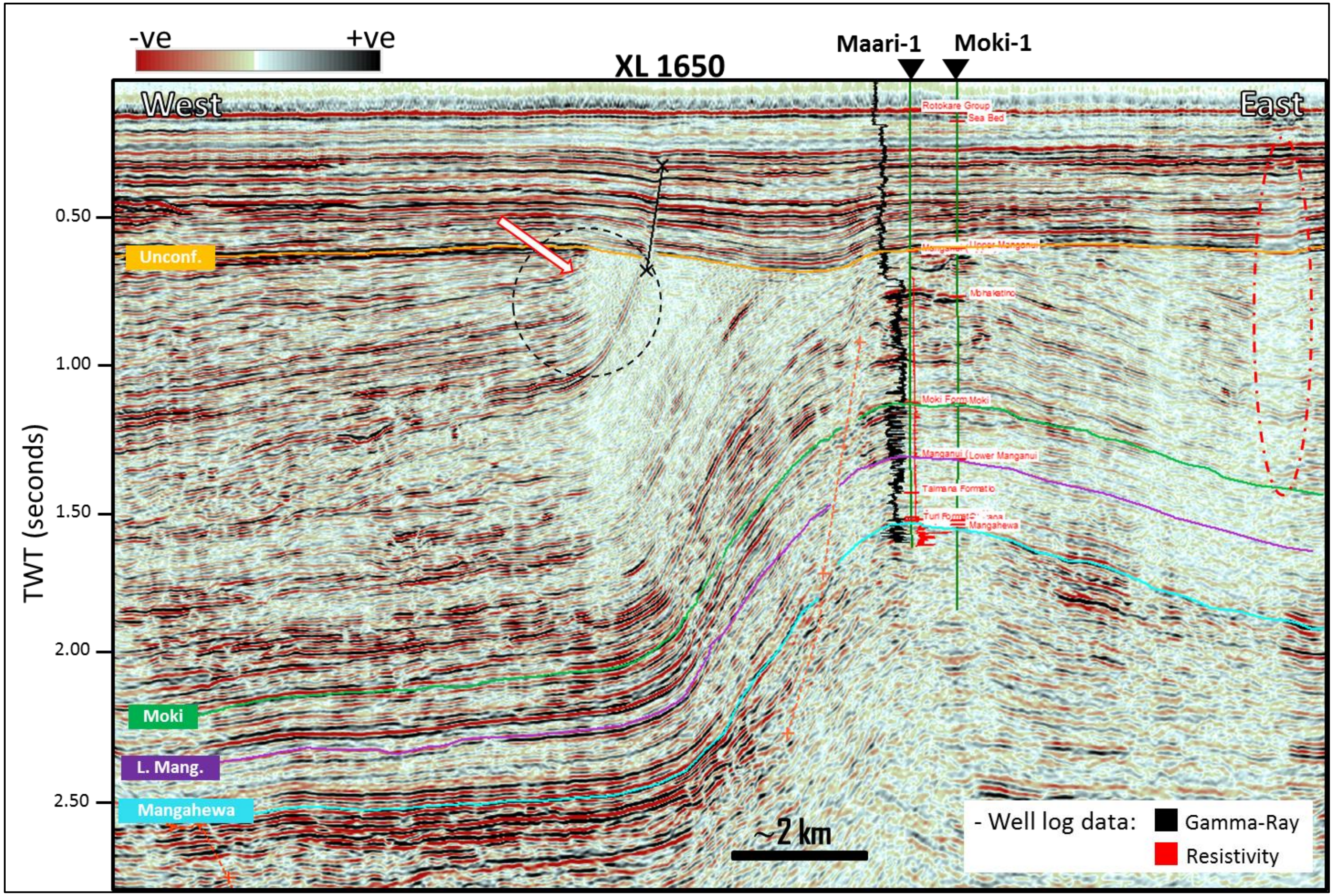

Figure 1.6: Seismic section on cross-line 1650. The red dashed ellipse shows a low amplitude zone possibly due to a shallow gas anomaly

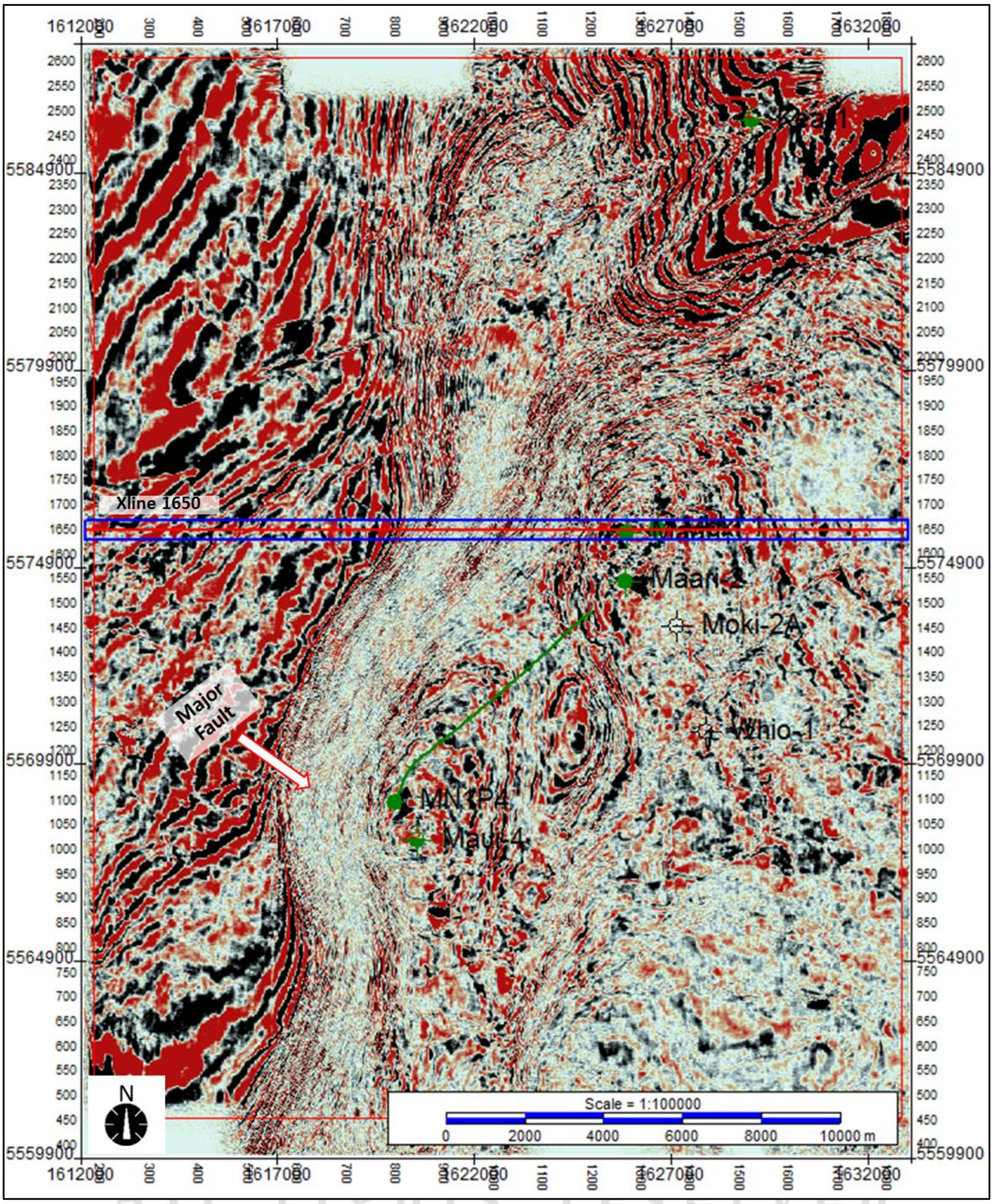

Figure 1.7: Time-slice at 850 ms TWTT, Maari 3D seismic data. Observe the large area with a lack of amplitudes due to a poor definition of the fault location. The reason for the imaging issue is that the strike direction of the inverted structure coincides with the direction that seismic was acquired (Inline direction)

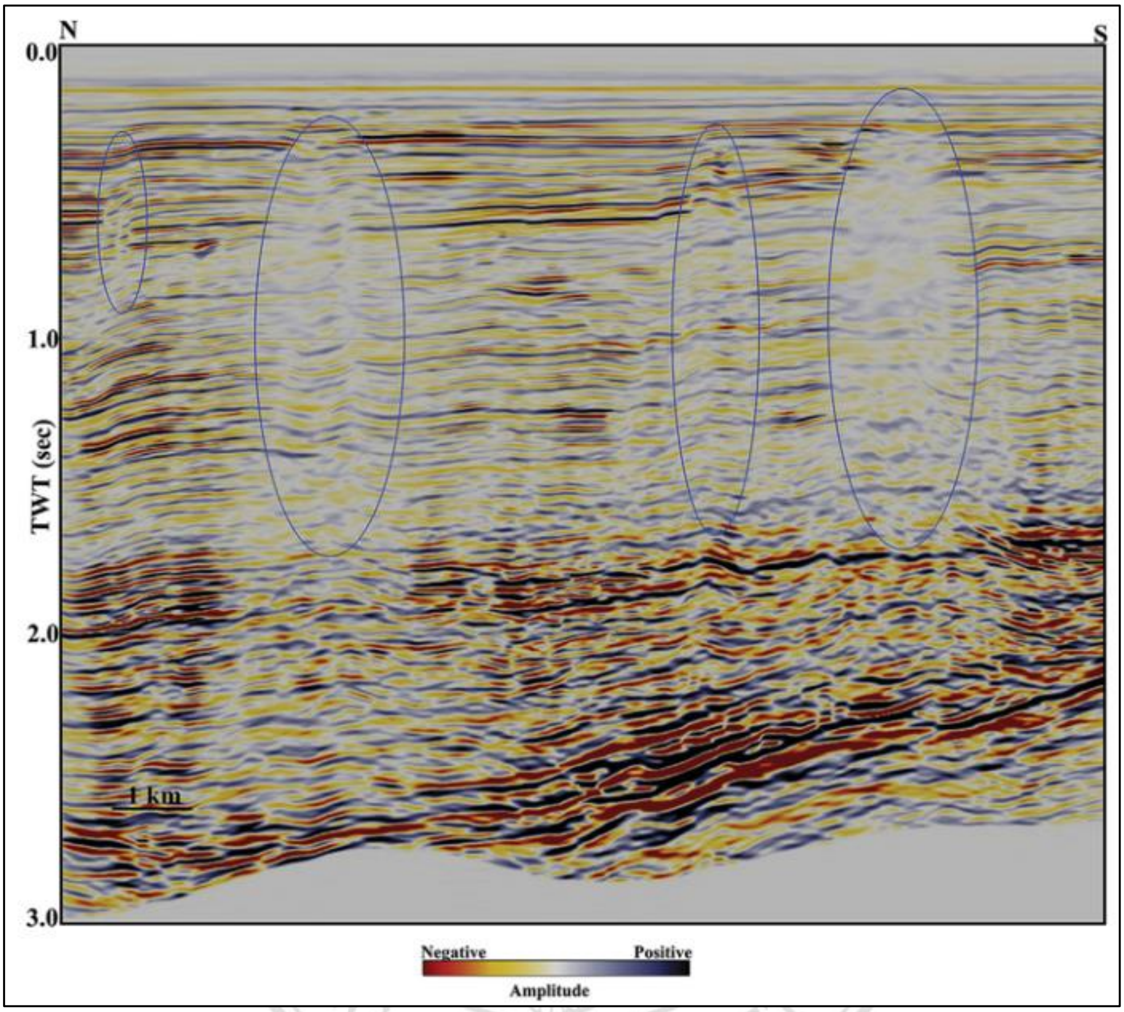

Figure 1.8: A dip-steered median filter (DSMF) section on inline 793 showing with the blue ellipses showing low amplitudes zones associated with gas chimneys (Singh *et al*., 2006)

1.3. Well Data

The current survey utilizes data from seven wells drilled in the Maari Field area. Each well contains a full suite of wireline logs, formation tops (markers) and check-shot or VSP (Vertical Seismic Profile) information. Table 1.2 displays a relation of the wells and their available well logs. The first exploration well in Maari area was drilled in 1970 – the Maui-4 well. It was drilled at the crest of the Manaia structure with the discovery of oil bearing sands within the Kapuni Group (de Bock *et al.*, 1991). In 1983, the Moki-1 well was drilled in the Moki structure, another anticline associated with an inversion zone. The well revealed a new discovery, this time at younger stratigraphic units: Moki Fm. and M2A sands. The Moki-2A well (1984) was drilled immediately after that to appraise the extent of the oil accumulation discovered by Moki-1. From there on, other prospects have been drilled in the area: Kea-1 well (1985), drilled at a fault-bound dip closure (dry hole) and Whio-1 (2015), drilled at the crest of a small anticline in the migration fairway from a proven Cretaceous source rock (dry hole). Development and appraisal wells were also drilled, case of the wells Maari-1 well (1998) and Maari-2 well (2003) drilled to test and investigate reservoir properties variation within the Moki sands.

Table 1.2 – Relation of available well logs at each well.

Wells	Available well logs
Kea-1	BS, CALI, DENS, DRHO, DTC, GR, NEUT, PEF, RESD, RESS, SP, TENS
Maari-1	BS, CALI, DENS, DRHO, DTC, DTS, GR, NEUT, PEF, RESD, RESS, SP, TEMP, TENS
Maari-2	BS, CALI, DENS, DRHO, DTC, DTS, GR, NEUT, PEF, RESD, RESM, RESS, TEMP, TENS
Maui-4	BS, CALI, DENS, DRHO, DTC, GR, NEUT, PEF, RESD, RESS, TEMP
Moki-1	BS, CALI, DENS, DRHO, DTC, GR, NEUT, PEF, RESD, RESS, SP, TENS
Moki-2A	BS, CALI, DENS, DRHO, DTC, GR, NEUT, RESD, RESS, SP, TEMP
Whio-1	BS, CALI, DENS, DRHO, DTC, DTS GR, NEUT, PEF, RESD, RESS, SP, TENS

BS – Bit Size, Cali – Caliper; DENS – Density; DRHO – Bulk Density Correction; DTC – Delta-T Compressional; DTS – Delta-T Shear; GR – Gamma Ray; NEUT – Neutron; PEF – Photoelectric Factor; RESD – Deep Resistivity; RESM – Medium Resistivity; RESS – Shallow Resistivity; SP – Spontaneous Potential; TEMP – Cartridge Temperature; TENS – Cable Tension

1.4. Literature Review

The estimation of Earth's properties from any measured seismic trace is known as Seismic Inversion (Yilmaz, 1987). The term Inversion - in a geophysical sense – is more general and can be defined as a procedure of obtaining subsurface models that may adequately describe an observed data set (Treitel and Lines, 1999). Seismic

Inversion is a technique that has been used by geophysicists for at least forty years. It started with the work of Backus and Gilbert (1967 and 1970) providing the theoretical foundation to extract layer properties from seismic records. In their approach, observed and synthetic seismic traces are matched through a suitable optimization algorithm that minimizes some measure of the difference between the observed and the computed data. Then Jackson (1972) brought attention to the fact that the solutions in the inversion process are not unique as an infinite number of solutions satisfy the data within determined error bounds.

After that, numerous inversion methods have been developed using different ways of constraining the range of solutions. Solutions are constrained by adding *a priori* knowledge about the subsurface parameters, which normally comes from well information. They can be either "hard", determined by geological possible output values for density and velocity, for instance, or they can be "soft" and expressed in the form of probability density functions which consequently estimate the probability density of solutions to a given inverse problem. That way, the most likely set of model parameter values are revealed. Tarantola (1987) was one of the first enthusiasts to defend the use of this probabilistic approach.

It was not until the 1990s with the advances in computational power that stochastic inversion started to be applied more often. In fact, the first successful application of geostatistics in seismic inversion was presented by Haas and Dubrule (1994). In this paper, they presented a methodology referred to as *Sequential Gaussian Simulation*, which is based on simulations to estimate an impedance value from its Gaussian distribution to a random seismic trace. Reflectivity coefficients are calculated and convolved with the wavelet until a satisfactory trace match is obtained. A single realisation is completed when all the traces have been inverted; the stochastic inversion is finished just when every choice from a constrained function has been tested by a realisation. Later on, other algorithms introducing new approaches to the geostatistical method were under development, mainly trying to reduce the computational expense. Grijalba-Cuenca *et al.* (2000) performed tests with a geostatistical inversion technique working on a grid-cell basis, instead of trace by trace. This algorithm estimated a local probability density function (PDF) from the PDF of the available control points by a kriging technique and also required stratigraphic and structural information as an input.

The final result is selected by a simulated annealing method (see Debbeye *et al.*, 1996) which operates accepting or rejecting a given simulation. Another method of stochatic inversion was presented by Francis (2005) and works based on a Fast Fourier Transform (FFT) based spectral simulation to generate impedance realisations, which are then conditioned to well impedance and seismic amplitude data. Finally, Naghaded *et al.* (2017) incorporated the work of Margrave *et al.* (2003), who developed a non-stationary deconvolution method (Gabor deconvolution), into a stochastic framework. This method removes the source wavelet effects from the seismic trace by extracting the time-variant wavelet properties. The estimated reflectivity will then present higher resolution and the bias incorporated by the well-log information (low-frequency and variogram model) will lead the stochastic Gabor inversion to accurately estimate absolute acoustic impedance values.

Since the late 1990's developments have been made regarding the integration of stochastic inversion results and rock physics information to be included in reservoir models (Saussus and Sams, 2012). Torres-Verdin *et al.* (1999) applied the stochastic inversion as a quantitative way of assessing the lateral extent of wireline petrophysical variables away from well locations. The study used post-stack seismic data from a producing field in the San Jose Basin, Argentina, and the main objective was to predict the extent of thin sand layers (thinner than seismic resolution) in order to guide reservoir engineers for field development drilling decisions. The authors concluded the results were consistent with fluid production data and proved the stochastic method's competence to deal with layers below seismic resolution as well as the non-uniqueness problem. In the same line of thought, Contreras *et* al. (2005) used pre-stack seismic data combined with well data to characterize flow units of a deep-water Miocene reservoir located in the Gulf of Mexico by applying AVA Stochastic inversion. The study combined rock/fluid information through Amplitude Versus Angle (AVA) seismic data with a co-simulation via lithotype-dependent probability distributions of petrophysical properties to create 3D reservoir models with considerably higher resolutions than those presented by deterministically inverted results. The authors highlighted that combining all of these methods with the existing geologic information can significantly reduce development risks, especially those associated with non-conventional reservoirs.

Also, comparisons between deterministic and stochastic methods results are frequently found in the literature, as for example Sancervero *et al.* (2005), Bosch and Gonzalez (2010), Watanabe (2013) and Wu (2015). Most of these works emphasize, with real data, evidence of the advantages of the stochastic over the deterministic. The ability to deal with the non-uniqueness problem of the sub-tuning component in seismic data is always mentioned. Recently, there has also been an increasing acknowledgement that the subsurface's heterogeneity is primordial in this field as it is strictly related to uncertainties in interpretation. Thus, many authors consider the attempt to quantify the variability of the inverse solution as one of the most important advances when it comes to reservoir modeling purposes.

1.5. Research Objectives

The main objective of the current study is to apply stochastic inversion to the 3D Maari seismic volume to estimate reservoir properties and predict lithology away from the well locations. In order to do this a series of steps must be carried out. These can be summarized as follow:

I. Invert the seismic data to acoustic impedance and relate this property to lithology/fluid changes around the field;
II. Evaluate the inversion results through the use of 'blind' wells;
III. Obtain relationships to estimate other reservoir properties from P-impedance volume.